Expanded View Figures

Figure EV1. Rediscovery of the chaperone Spy by using Tn-Seq.

A Transposon insertions resistant to 1.5 mg/ml of ampicillin were selected in both the wild-type strain MG1655 and its isogenic *baeS*-R426S derivative; both strains harbored the plasmid pBR322. Both of these strains were significantly ampicillin sensitive at this ampicillin concentration, showing about one log of killing (see Appendix Fig S1). An overall decrease in the number of transposon insertions in the wild-type strain MG1655 in the presence of ampicillin was observed, likely reflecting the ~1 log killing induced by the antibiotic, but there is no substantial decrease in insertions the *spy* and *baeSR* genes relative to adjacent genes.

B Transposon insertion libraries selected on 0.7 and 1.2 mg/ml of ampicillin, respectively, were made in the MG1655 wild-type and *baeS*-R426S strains harboring a protein folding sensor pBR322 *bla*::Im7 L53A I54A. A dramatic decrease in transposon insertions in the *spy* and *baeSR* genes was observed in the *baeS*-R426S mutant strain relative to the insertion frequency found in wild-type strains, consistent with the known role of Spy, which is overproduced in the *baeS*-R426S strain, in stabilizing the Im7 portion of the folding biosensor.

 © 2020 The Authors

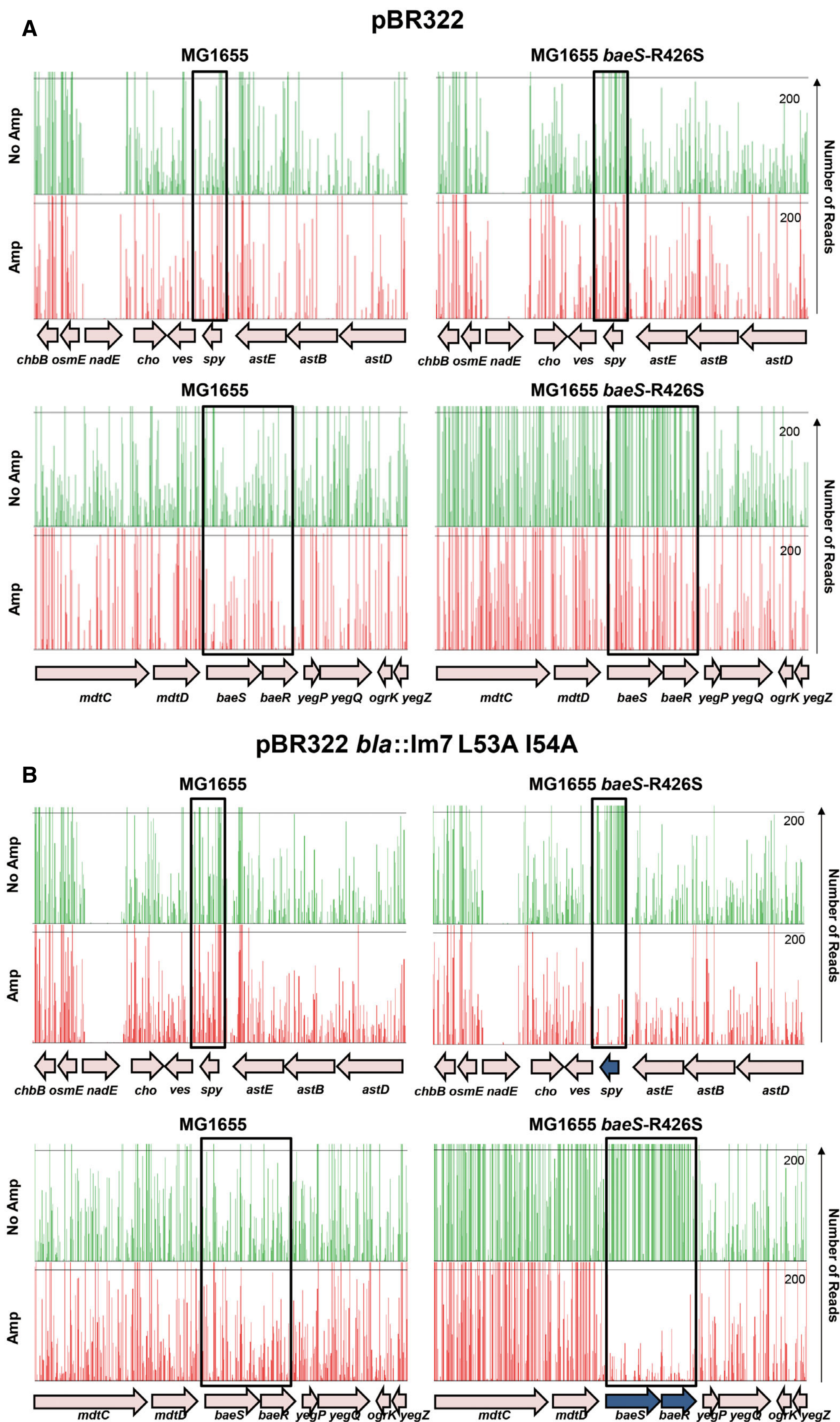

Figure EV1.

Figure EV2. UgpB inhibits CHO-induced protein aggregation more effectively when in the G3P-free form.

A–C (A) $UgpB_{G3P}$, which has ~90% G3P binding occupancy, was mixed with MDH incubated in 40 mM KH_2PO_4 KOH pH 7.5 buffer in the presence of 15 mM CHO at 37°C for 60 min and then centrifuged at 16,000 *g* for 20 min at 4°C to separate soluble and insoluble fractions (see Materials and Methods). Similar experiments were performed with G3P-free UgpB (B) and MBP (C). 12 μM MDH was used, and 1:1, 1:2, 1:4, 1:5, and 1:10 molar ratios of MDH:$UgpB_{G3P}$/UgpB/MBP were used.

D A similar experiment was performed using 800 μg of *E. coli* total lysate; 60 μM of $UgpB_{G3P}$/UgpB were used for the supernatant/pellet assay.

E 12 μM of MDH and a 1:1 ratio of UgpB:MDH were used for the CHO-induced aggregation assay. 15 mM CHO was used, and the mixtures were incubated at 37°C. At 30 min, the 120 μM, 1.2 mM, and 2.4 mM of G3P were added to the solutions containing the described proteins. After further 30-min incubation, soluble and insoluble fractions were separated (see Materials and Methods). Overall, experiment setting is same as Fig 6D. The solubility of MDH or UgpB itself is not affected by the addition of G3P. The addition of G3P into MDH and UgpB mixture leads the aggregation of MDH, suggesting G3P compete with MDH. Of note, UgpB is also aggregated to some extent. This result may suggest that UgpB is vulnerable to CHO exposure during the dissociation step.

Data information: These experiments were repeated twice with similar results, and one representative is shown.

© 2020 The Authors

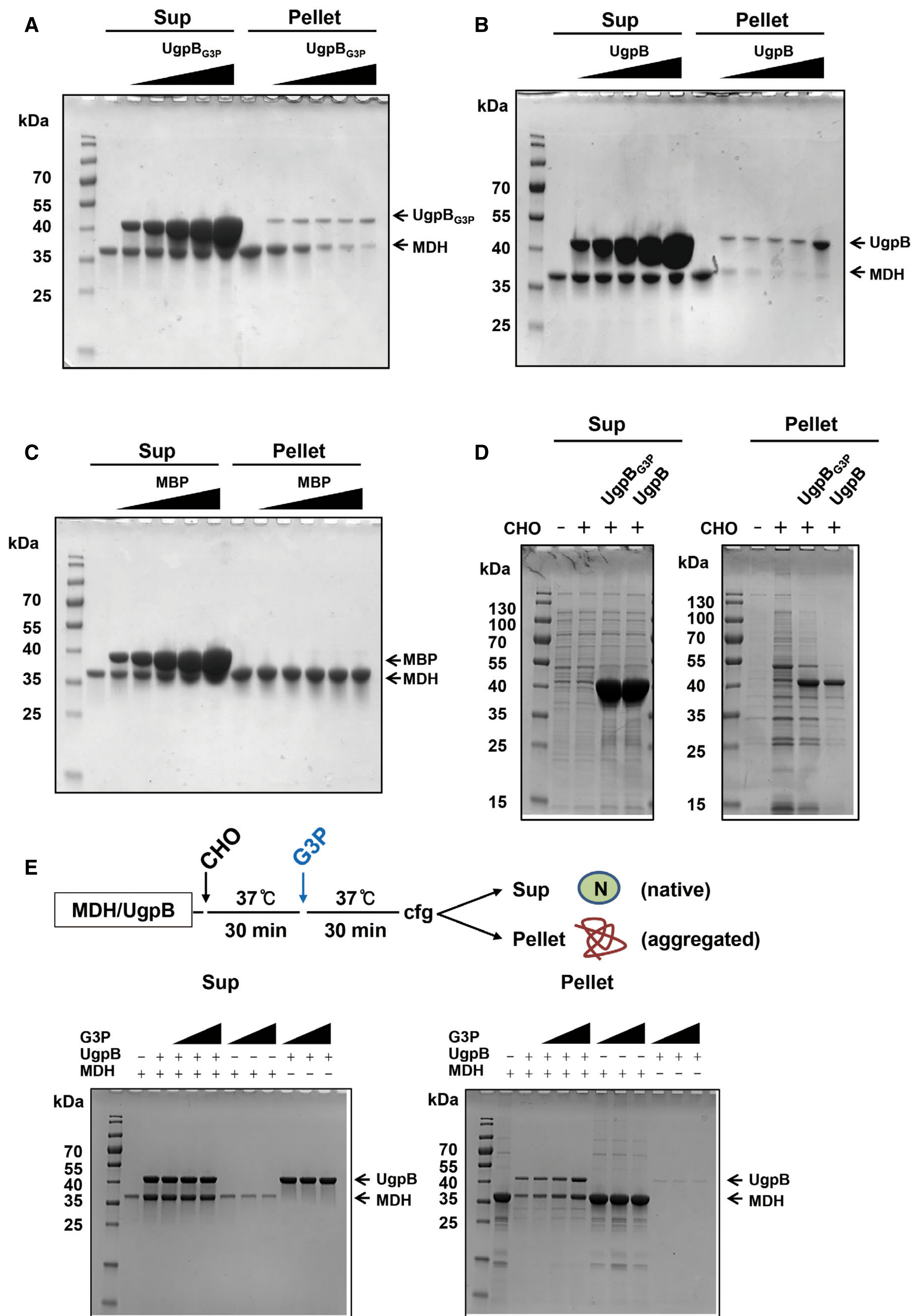

Figure EV2.

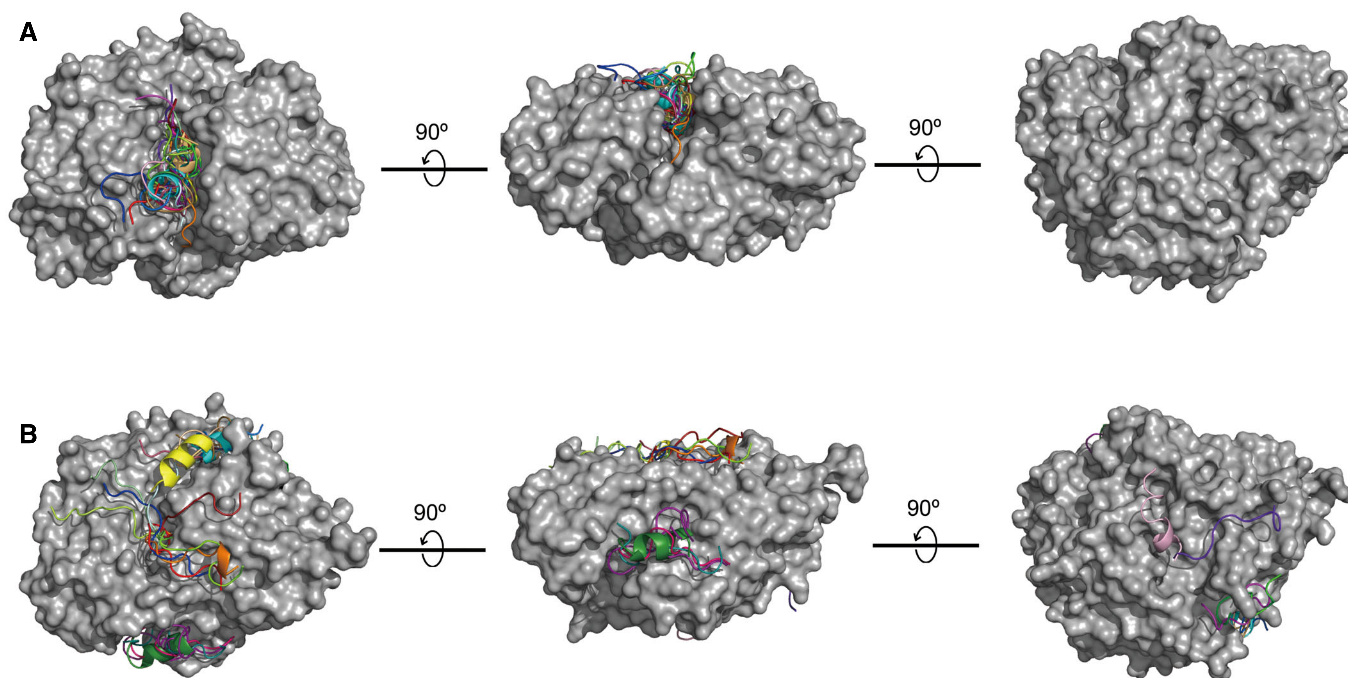

Figure EV3. Docking results for 24 different MDH peptides binding to UgpB.

A, B The best docked models with the lowest energy score for each peptide-docking complex with (A) apo UgpB and (B) holo UgpB are shown. Peptide sequence information and energy score are described in Dataset EV2.

 © 2020 The Authors

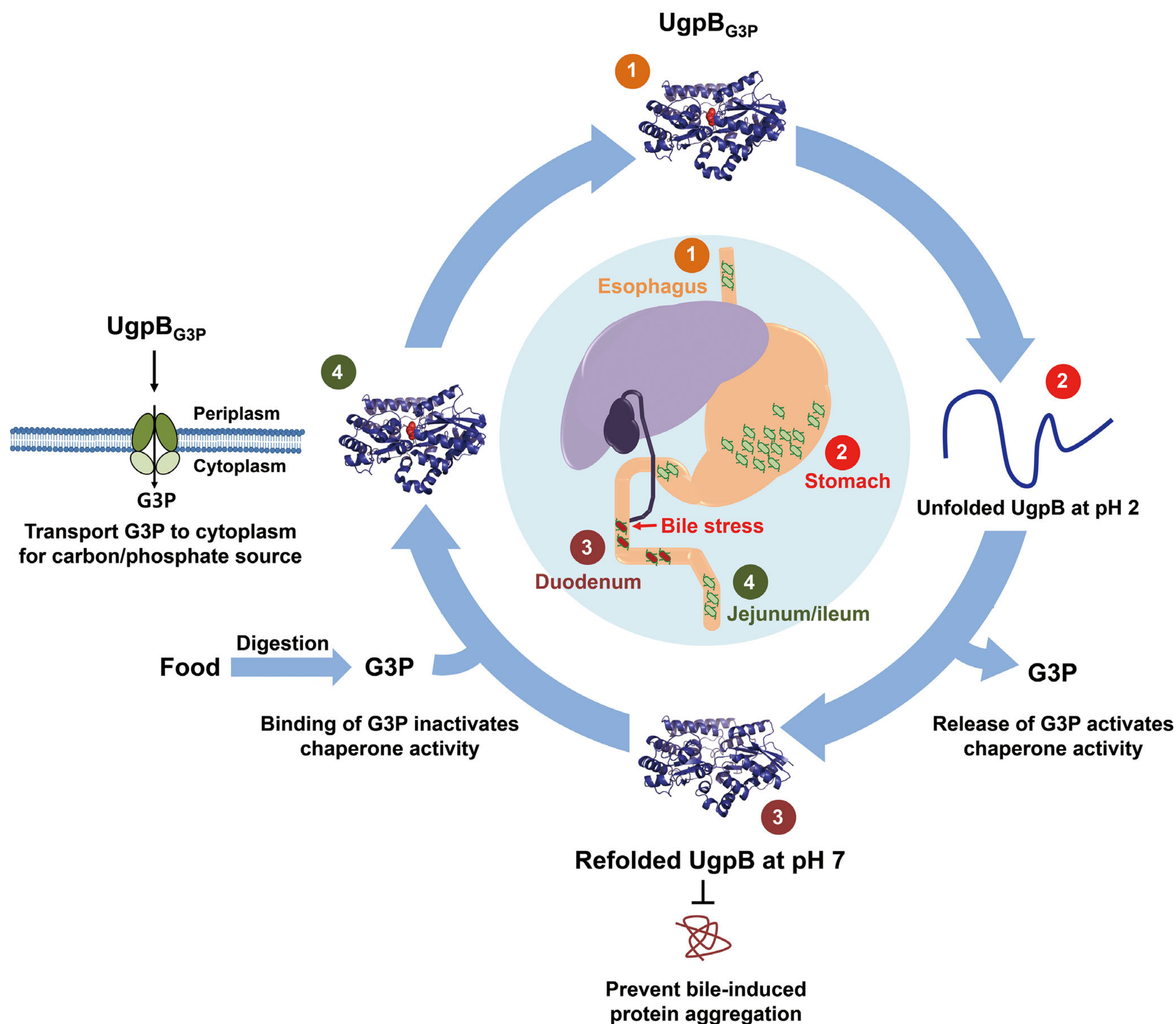

Figure EV4. Speculative model of UgpB in the digestive tract.

Enteric bacteria encounter host defense systems including gastric acid in the stomach and bile salts in the duodenum. Periplasmic UgpB unfolds in response to low pH present in the stomach, releasing any bound G3P. This activates UgpB as a molecular chaperone, allowing it to protect periplasmic proteins from the bile-induced aggregation in the duodenum. Upon transition into the jejunum and ileum, the bile concentration declines (Heaton, 1969; Weski & Ehrmann, 2012), and digestion of food substances increases G3P levels. These increasing G3P levels inactivate UgpB as a molecular chaperone, and it transitions into its role as a periplasmic G3P-binding protein, which helps to transport G3P into the cytosol.

© 2020 The Authors